N82 23461

Profiles of electrified drops and bubbles

O. A. Basaran and L. E. Scriven

Department of Chemical Engineering & Materials Science,
University of Minnesota, Minneapolis, Minnesota 55455

Abstract

Axisymmetric equilibrium shapes of conducting drops and bubbles, (1) pendant or sessile on one face of a circular parallel-plate capacitor or (2) free and surface-charged, are found by solving simultaneously the free-boundary problem consisting of the augmented Young-Laplace equation for surface shape and the Laplace equation for electrostatic field, given the surface potential. The problem is nonlinear and the method is a finite element algorithm employing Newton iteration, a modified frontal solver, and triangular as well as quadrilateral tessellations of the domain exterior to the drop in order to facilitate refined analysis of sharply curved drop tips seen in experiments. The stability limit predicted by this computer-aided theoretical analysis agrees well with experiments of Wilson and Taylor (1925). The instability and mechanism of charged droplet ejection are under theoretical and experimental study.

1. Introduction

The shape of a conducting fluid interface is affected by mobile surface charge. The distribution of mobile free, surface charge is affected in turn by the shape of the interface. At equilibri charge distributes to make uniform the potential of the interface. But surface charge creates an electrical pressure that competes with capillary pressure (the resultant of surface tension in a curved interface) and hydrostatic pressure to control the shape.

Only cylindrical and spherical equilibrium drops have yielded to classical analysis (Rayleigh 1882, Basset 1894, Taylor 1969, Michael and O'Neill 1972). Shapes that depart from standard coordinate surfaces can be analyzed by modern computer-aided mathematics with finite element basis functions (Gifford 1979).

Observations of electrified drops and bubbles stand in need of accurate retical analysis of shapes and stability. Free drops were studied by Nolan 1926, Macky 1931, Doyle, Moffett and Vonnegut 1964, and others; supported drops, by Zeleny 1914, 1917, Wilson and Taylor 1925, Macky 1930, Krohn 1974, and others. The results of analysis will pertain to such fields as spray generation in technology and cloud physics in science.

2. Observations of charged sessile soap-bubbles

A soap-bubble sitting on the lower, wetted plate of a circular parallel-plate capacitor appears hemispherical in the absence of field. As the field strength is raised the bubble elongates along the field direction. Because the plate is wetted the circular contact line slides freely and the contact angle remains approximately 90°. The prolate shape sequence seen at field strengths up to a critical value is a family of stable equilibrium shapes: four members are shown in Fig. 1. Computer-aided theoretical analysis is used to track this shape family in section 6.

Increasing the field strength even slightly beyond the critical value leads to a dynamic succession. The end of the bubble rapidly narrows and becomes conical. Filaments are subsequently ejected from the end of the bubble, this spitting being accompanied by intense vibrations of the tip. Such observations were originally reported by Wilson and Taylor (1925) and Macky (1930).

3. Statement of the two cases analyzed

The two situations treated here are shown in Fig. 2:
Case 1.
Axisymmetric drop or bubble sessile (pendant) on one face of a circular parallel-plate capacitor (Fig. 2a).
Case 2.
Free surface-charged drop in absence of an external imposed field (Fig. 2b).

4. Governing dimensionless groups, equations and boundary conditions

The relevant dimensionless groups are compiled in Table 1. In the case of the free

drops we choose to work with the potential at the drop surface relative to "infinity" instead of specifying the charge on the drop. The two alternatives are of course fully equivalent.

The governing equations of electrostatics and capillary hydrostatics and boundary conditions are summarized in Figs. 3 and 4. U is of course the electrostatic potential. In the normal stress balances at the interfaces 2H is twice the dimensionless mean curvature, a nonlinear function of first and second derivatives of the drop profiles; K is a reference pressure, E^2 represents the electrical pressure created by surface charge, and 4 Gz is the hydrostatic pressure created by a gravitational field (supposed absent in Case 2).

5. Computer-aided analysis

Theoretical computation of drop shape requires solving a system made nonlinear by the free boundary and by the curvature and electrical pressure in the augmented Young-Laplace equation. The procedure is:

(i) Estimate drop shape and electrostatic potential from *either* an analysis of limiting case *or* experimental observation.

(ii) Partition, or tessellate, the one-dimensional domain (drop profile) into curve segments and the two-dimensional domain (surrounding space) into quadrilaterals between *spines* θ = constant (cf. Kistler 1981) as indicated in Fig. 5.

(iii) In the 2-D domain construct finite element basis functions $\Psi^i(r,\theta)$ for the subdomain around each node:
- choose the biquadratic polynomial on the (ε,η)-unit square;
- map each quadrilateral isoparametrically onto the unit square (Fig. 6).

(iv) In the 1-D domain exploit the fact that the 1-D basis functions $\phi^i(\theta)$ when mapped isoparametrically onto $0 \le \varepsilon \le 1$ are simply and very conveniently the isoparametrically mapped $\Psi^i(\varepsilon,\eta = 0)$ (cf. Kistler 1981).

(v) Approximate the interface shape as

$$f(\theta) = \sum_{i=1}^{M} q_i \phi^i [\theta(\varepsilon)]$$

and the potential as

$$U(r,\theta) = \sum_{i=1}^{N} U_i \Psi^i [r(\varepsilon,\eta), \theta(\varepsilon,\eta)].$$

(vi) Form Galerkin weighted residuals and require them to vanish

(vii) Solve the resulting $N + M + 1$ nonlinear algebraic equations for the unknown coefficients (q_i, U_i, K) by Newton iteration:
- derivatives with respect to q_i's are calculated by ganging nodes along spines;
- the domain is updated at each iteration;
- convergence approaches quadratic rate;
- the Jacobian is valuable for continuation in the parameters and evaluation of stability.

(viii) Modify the frontal solver (Irons 1970, Hood 1976, 1977) to handle the constraint of fixed volume and use it for the linear equation set in Newton iteration.
- The presence of a free boundary makes the frontal solver cost-effective.

(ix) Terminate iteration when the norm of the largest component of correction vector is sufficiently small.

(x) Change the parameter (typically E_∞ or U_o), estimate a shape by continuation and begin anew.
- Prefer the secant version of first-order continuation because it is easier to use than the tangent version and it maintains near-quadratic convergence with bigger parameter changes than does zeroth-order continuation.

(xi) *Concentrate computational power where needed:*
- refine the tessellation in regions of sharp gradients;
- derive Robin boundary condition to account for asymptotic far field behavior and thereby shrink the computational domain.

An example of the last point is shown in Fig. 7: a finite element mesh of triangles and rectangles which proved computationally efficient.

6. Results

Calculations were programmed in FORTRAN and made on the Control Data Corporation CYBER 74 at the University of Minnesota. 3 sec/iteration was typical for $N + M + 1 = 183$ unknowns and 2 - 4 iterations were required to converge.

Case 1. Results for axisymmetric supported bubble (G = 0)

Finite element calculations for a bubble meeting one of the capacitor plates at a fixed contact angle of 90° simulate theoretically experiments with electrified soap-bubbles

described in section 2 (cf. Wilson and Taylor 1925 and Macky 1930). Moreover, if the spacing between the plates is much larger than the bubble radius, both experiment and theory model a drop freely floating in a uniform applied electric field in the absence of gravity. Drop shapes and equipotentials for a bubble of volume $2\pi/3$ are plotted as function of the parallel-plate electric field E_∞ in Fig. 8, which shows that bubble profiles are prolate in the field direction. This theoretical analysis using finite element basis functions can be made as accurate as the computer allows and it already confirms Taylor's (1964) spheroidal approximation.

Results for a bubble of volume $2\pi/3$ with its contact line fixed are plotted in Fig. 9. The theoretical analysis predicts that bubble shape tends toward conical.

Families of drops of volume $2\pi/3$ with either the contact line fixed or the contact angle prescribed are plotted in parameter space in Fig. 10. In both cases the family loses stability at a turning point, bubbles with contact line fixed being the more stable of the two. The stability limit predicted for the fixed contact angle case by this computer-aided theoretical analysis is within 3% of the value 0.321 obtained experimentally by Wilson and Taylor (1925).

Aspect ratio as function of parallel-plate electric field E_∞ is plotted in Fig. 11. When contact angle is fixed the critical bubble is elongated 1.82/1.37 times as much as one with contact line fixed.

How surface charge distributes on supported bubbles is plotted in Fig. 12. The ordinate is the ratio of local surface charge density on the bubble to charge density on the plate far from the bubble. Because electrical pressures goes as the square of charge density, electrical pressure at the bubble tip attains values from 40 to 50 times as large as that between two parallel-plates for the larger of the two voltages shown.

Case 2. Results for axisymmetric free surface-charged drop

Though the sphere is an equilibrium shape at all values of charge q it was shown by Lord Rayleigh (1882; see also Hendricks and Schneider 1962) that a sphere of radius R is unstable to any perturbation proportional to the Legendre polynomial of order n, $P_n(\cos\theta)$, if the charge exceeds

$$q > 4\pi\sqrt{(n+2)\,\varepsilon_o \sigma R^3}$$

or, in dimensionless form,

$$Q > 2\pi\sqrt{2(n+2)} \qquad or \qquad U_o > \sqrt{\frac{n+2}{2}}$$

Instability first appears for the $n = 2$ mode, i.e. the second spherical harmonic, and the criteria $Q = 4\pi\sqrt{2}$ or $U_o = \sqrt{2}$ are known as the Rayleigh limit. The finite element analysis predicts the first instability to occur at $U_o = 1.42$, which is in good agreement with the value $\sqrt{2}$, and to correspond to bifurcation from the trunk family of spheres (Fig. 13). The theoretical analysis also reveals that bifurcation at the Rayleigh limit is *subcritical*, thereby confirming Taylor's (1964) surmise from his spheroidal approximation. A secondary bifurcation is found at $U_o = 1.40$ along this branch family of prolate shapes. The theoretical analysis accurately predicts the bifurcation points of the higher modes, but these are not shown in Fig. 13.

7. Concluding Remarks

Charge repulsion can overcome the attractive-like action of surface tension and when it does it limits the surface charge that can be stably carried by a fluid interface: at the limiting charge density the interface becomes unstable.

Computer-aided analysis with finite element basis functions can handle relatively complicated equilibrium profiles of electrified drops. The finite element algorithm developed here is not limited in its applicability in contrast to the method of Borzabadi and Bailey (1978), who calculated profiles of drops hanging from a tube connected to a high voltage source.

Additional results will be reported elsewhere. With the flow field inside the drop accounted for, the methods developed here and certain others should make it possible to analyze the dynamic succession in unstable drops and settle the long-standing question of how charged drops break up.

Acknowledgments

The authors would like to thank K. A. Amundson for assisting with the construction of the parallel-plate capacitor and taking the photographs, and R. E. Benner, N. E. Bixler and S. F. Kistler for extensive discussion and valuable insights into finite element analysis of free boundary problems. This research was supported by NASA Fund for Independent Research.

References

A. B. Basset, Waves and Jets in a Viscous Liquid, *Am. J. Math.* 16 13 (1894).

E. Borzabadi and A. G. Bailey, The Profiles of Axially Symmetric Electrified Pendent Drops, *J. Electrostatics* 5 369 (1978).

A. Doyle, D. P. Moffett, and B. Vonnegut, Behavior of Evaporating Electrically Charged Droplets, *J. Colloid Sci.* 19 136 (1964).

W. A. Gifford, The Shapes and Stability of Charged, Rotating Liquid Drops, Ph.D. Thesis, University of Minnesota (1979).

C. D. Hendricks and J. M. Schneider, Stability of a Conducting Droplet Under the Influence of Surface Tension and Electrostatic Forces, *Am. J. Phy.* 31 450 (1962).

P. Hood, Frontal Solution Program for Unsymmetric Matrices, *Int. J. Num. Meth. Engng.* 10 379 (1976).

P. Hood, Note on Frontal Solution Program for Unsymmetric Matrices, *Int. J. Num. Meth. Engng.* 11 1055 (1977).

B. M. Irons, A Frontal Solution Program for Finite Element Analysis, *Int. J. Num. Meth. Engng.* 2 5 (1970).

S. F. Kistler, First International Fluid Mechanics Winter (Summer) Seminar, INTEC-Santa Fe, 18-21 August 1981.

V. E. Krohn, Electrohydrodynamic Capillary Source of Ions and Charged Droplets, *J. App. Phy.* 45 1144 (1974).

W. A. Macky, The Deformation of Soap-Bubbles in Electric Fields, *Proc. Camb. Phil. Soc.* 26 421 (1930).

W. A. Macky, Some Investigations of the Deformation and Breaking of Water Drops in Strong Electric Fields, *Proc. Roy. Soc. Lond.* A133 565 (1931).

D. H. Michael and M. E. O'Neill, The Bursting of a Charged Cylindrical Film, *Proc. Roy. Soc. Lond.* A328 529 (1972).

J. J. Nolan, The Breaking of Water-Drops by Electric Fields, *Proc. Roy. Irish Acad.* 37 28 (1926).

Lord Rayleigh, On the Equilibrium of Liquid Conducting Masses Charged with Electricity, *Phil. Mag.* 14 184 (1882).

G. I. Taylor, Disintegration of Water Drops in an Electric Field, *Proc. Roy. Soc. Lond.* A280 383 (1964).

G. I. Taylor, Electrically Driven Jets, *Proc. Roy. Soc. Lond.* A313 453 (1969).

C. T. R. Wilson and G. I. Taylor, The Bursting of Soap-Bubbles in a Uniform Electric Field, *Proc. Camb. Phil. Soc.* 22 728 (1925).

J. Zeleny, On the Conditions of Instability of Electrified Drops, with Applications to the Electrical Discharge from Liquid Points, *Proc. Camb. Phil. Soc.* 18 71 (1914).

J. Zeleny, Instability of Electrified Liquid Surfaces, *Phys. Rev.* 10 1 (1917).

TABLE 1

Governing dimensionless groups

SUPPORTED DROP	FREE DROP
E_∞ = PARALLEL-PLATE ELECTRIC FIELD, $(\frac{\epsilon_0 R}{2\sigma})^{1/2}\frac{u_0}{h}$	U_0 = POTENTIAL AT DROP SURFACE WITH RESPECT TO INFINITY, $(\frac{\epsilon_0}{2\sigma R})^{1/2} u_0$
G = GRAVITATIONAL BOND NUMBER, $\frac{R^2 \Delta\rho g}{4\sigma}$	Q = NET CHARGE ON DROP, $(\frac{1}{2\epsilon_0 R\sigma})^{1/2} q$
R = *EITHER* RADIUS OF CONTACT CIRCLE *OR* RADIUS OF HEMISPHERE OF EQUAL VOLUME (SPECIFIED CONTACT ANGLE CASE)	R = RADIUS OF SPHERE OF EQUAL VOLUME
$\Delta\rho$ = DENSITY DIFFERENCE BETWEEN SURROUNDINGS AND DROP	
K = DATUM PRESSURE DIFFERENCE, $(p - p_{axis})\, R/\sigma$ AT $z = 0$	K = EXCESS DROP PRESSURE OVER AMBIENT PRESSURE, $(p - p_{amb})\, R/\sigma$

ϵ_0 = PERMITTIVITY OF FREE SPACE, σ = SURFACE TENSION

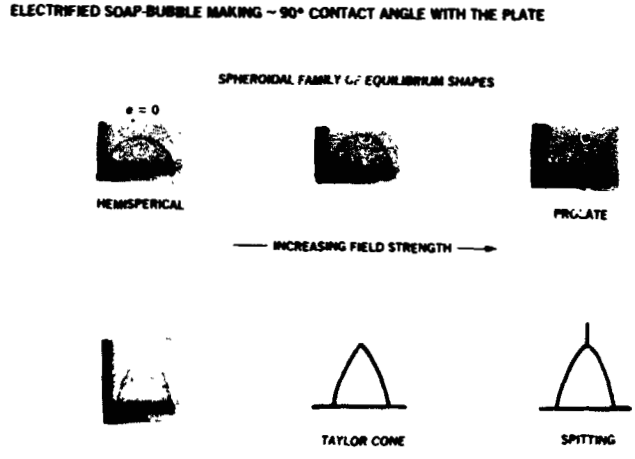

Figure 1. Observations of a charged sessile soap-bubble.

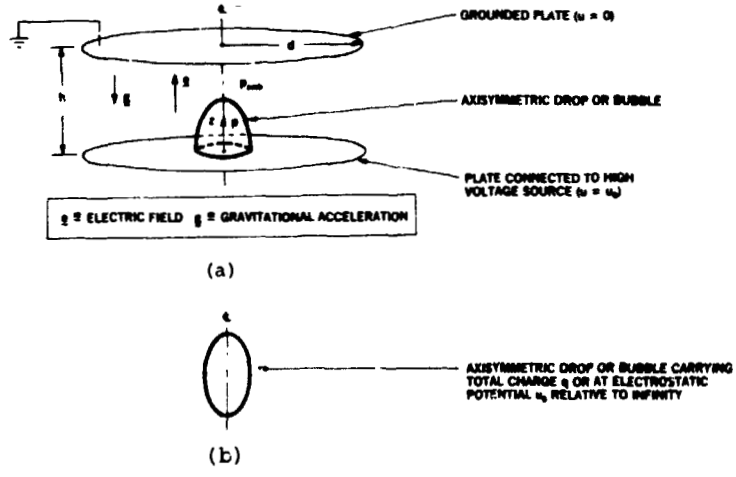

Figure 2. (a) Axisymmetric drop or bubble sessile (pendant) on one face of a circular parallel-plate capacitor; (b) free surface-charged drop (no applied field).

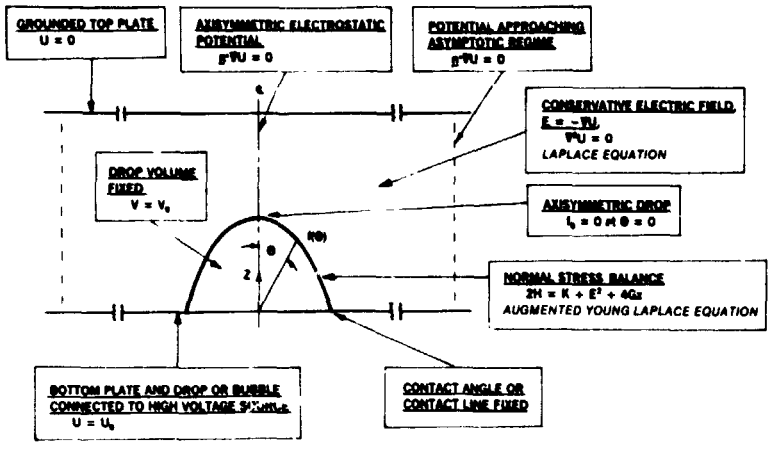

Figure 3. Governing equations and boundary conditions (Case 1).

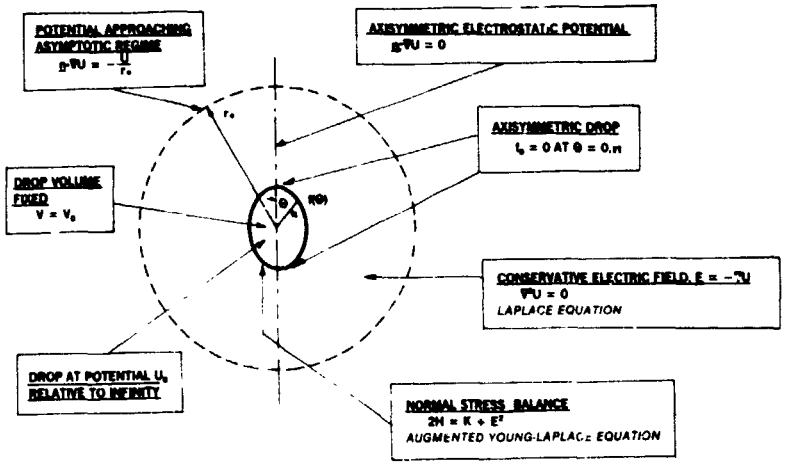

Figure 4. Governing equations and boundary conditions (Case 2).

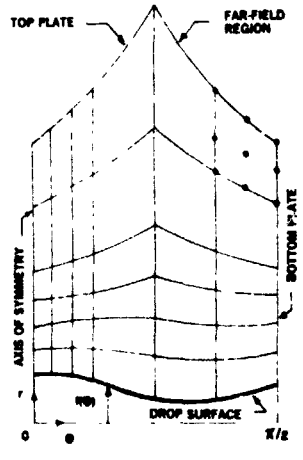

Figure 5. Spherical coordinate representation.

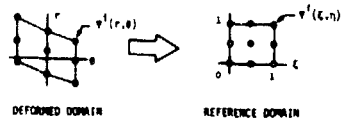

Figure 6 Isoparametric mapping, i.e. mapping by the polynomial function of the finite element function itself

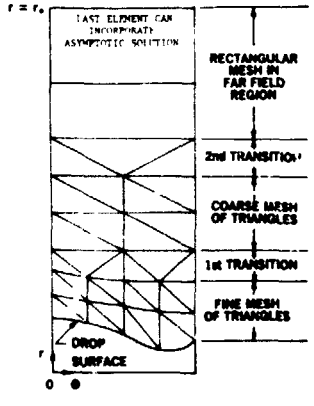

Figure 7 Computationally efficient finite element mesh for electrified drop problems

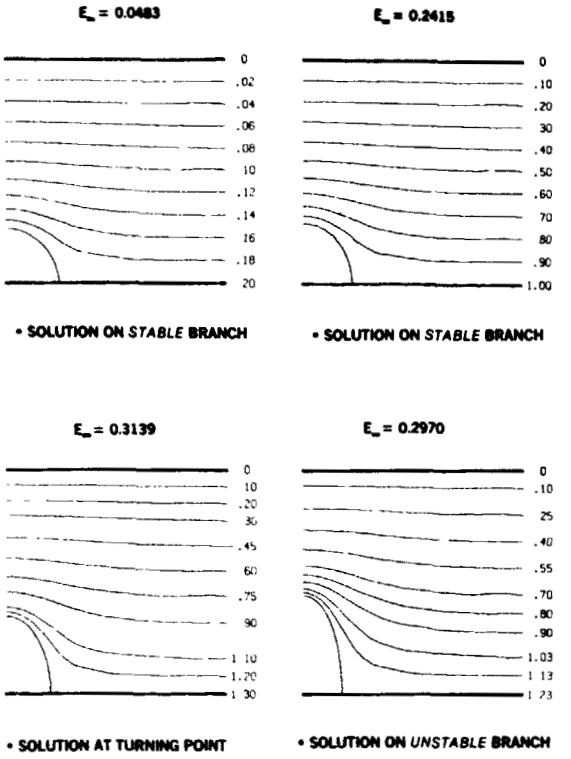

Figure 8. Drop shapes and equipotentials for fixed contact angle (90°) case.

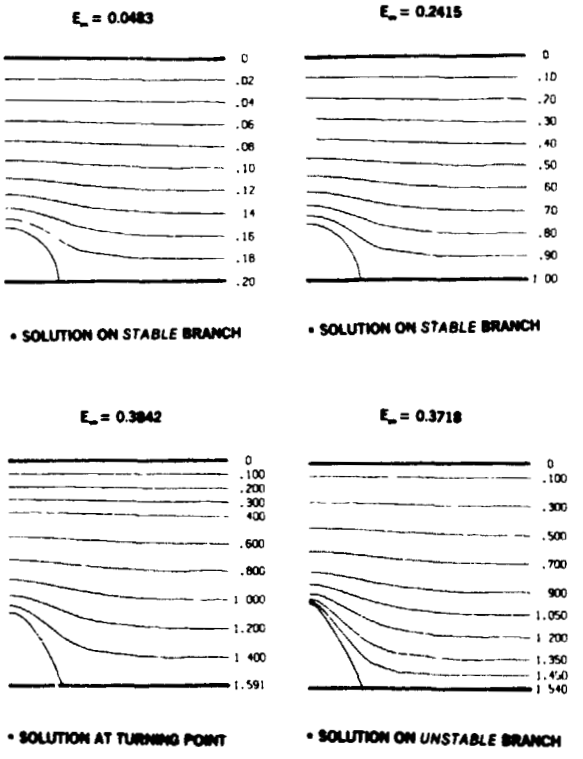

Figure 9. Drop shapes and equipotentials for fixed contact line case.

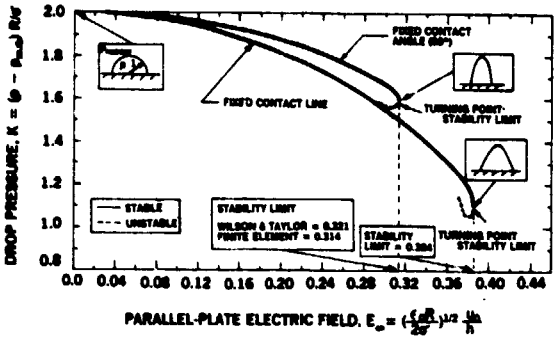

Figure 10. Solution families in parameter space for axisymmetric supported bubble (G = 0).

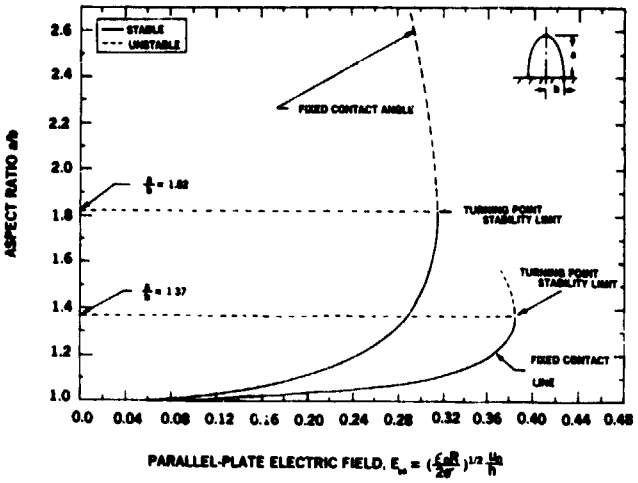

Figure 11. Aspect ratio a/b as a function of parallel-plate electric field E_∞.

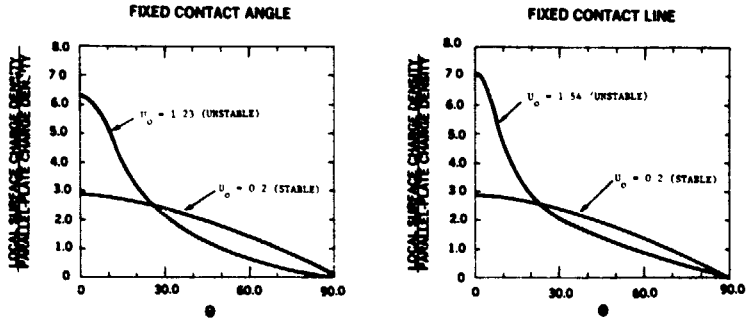

Figure 12. Distribution of surface charge on sessile bubbles.

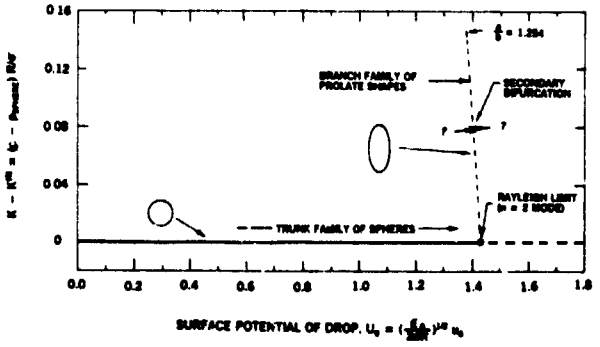

Figure 13. Bifurcation diagram in parameter space for free surface-charged drop (no externally applied field).